

QUANTITATIVE COMPARISON OF PERMEABILITY IN THE ADHESIVE INTERFACE OF FOUR ADHESIVE SYSTEMS

Juhea Chang¹, Keewook Yi², Hae-Young Kim³, In Bog Lee¹, Byeong Hoon Cho¹, Ho-Hyun Son^{1*}

¹*Department of Conservative Dentistry and Dental Research Institute, School of Dentistry, Seoul National University*

²*Geochronology Team, Korea Basic Science Institute*

³*Craniomaxillofacial Life Science(BK 21), School of Dentistry, Seoul National University*

ABSTRACT

The purpose of this study was to perform quantitative comparisons of water permeable zones in both the adhesive and the hybrid layer before and after thermocycling in order to assess the integrity of the bonding interface. Twenty eight flat dentin surfaces were bonded with a light-cured composite resin using one of four commercial adhesives [OptiBond FL (OP), AdheSE (AD), Clearfil SE Bond (CL), and Xeno III (XE)]. These were sectioned into halves and subsequently cut to yield 2-mm thick specimens; one specimen for control and the other subjected to thermocycling for 10,000 cycles. After specimens were immersed in ammoniacal silver nitrate for 24 h and exposed to a photo developing solution for 8 h, the bonded interface was analyzed by scanning electron microscopy (SEM) and wavelength dispersive spectrometry (WDS) at five locations per specimen. Immediately after bonding, the adhesive layer of OP showed the lowest silver uptake, followed by CL, AD, and XE in ascending order ($p < 0.0001$); the hybrid layer of CL had the lowest silver content among the groups ($p = 0.0039$). After thermocycling, none of the adhesives manifested a significant increase of silver in either the adhesive or the hybrid layer. SEM demonstrated the characteristic silver penetrated patterns within the interface. It was observed that integrity of bonding was well maintained in OP and CL throughout the thermocycling process. Adhesive-tooth interfaces are vulnerable to hydrolytic degradation and its permeability varies in different adhesive systems, which may be clinically related to the restoration longevity. [J Kor Acad Cons Dent 34(1):51-61, 2009]

Key words: Dentin, Adhesive, SEM, WDS, Thermocycling, Permeability

- Received 2008.11.26., revised 2008.12.31., accepted 2009.1.2-

I . INTRODUCTION

Since the acid-etch technique for bonding to the tooth substrate had been introduced, adhesive dentistry evolved rapidly due to two main reasons: esthetic satisfaction and minimal invasiveness. Some retrospective clinical studies have showed the favorable durability of resin restoration over 10 years^{1,2)}. However, the majority of bonded restorations are disadvantaged by their early failure during service and

they only remain in an optimum condition for a limited period of time. Generally, the immediate bonding effectiveness of current dentin adhesives seems to be favorable, but their potential degradation process is still a concern^{3,4)}. Recent studies have identified the major factors affecting durability as the hydrolysis of interface components such as collagen and resin, and subsequent elution of the breakdown products⁵⁾.

Currently, increased permeability of hydrophilic adhesive systems showed water uptake within the adhesive resin matrix, leading to incomplete polymerization⁶⁾. In the bonding process, unbound monomers or additives in the nanoleakage spaces are extracted by solvents. Following this, leachable components can be created in the aqueous environment over time. Thermocycling is a widely used artificial aging

* Corresponding Author: **Ho-Hyun Son**
 Dept of Conservative Dentistry,
 School of Dentistry, Seoul National University
 28 Yeongon-dong, Jongno-gu, Seoul, Korea
 Tel: 82-2-2072-2652 Fax: 82-2-2072-3859
 E-mail: hhson@snu.ac.kr

methodology. The water storage and the changing temperature closely simulate the actual environment within the oral cavity⁷⁾.

Microscopic observations of deficient margins have been presented with quantified measurements of leakage in various ways. One of the most popular methods provides scores for each scale for severity of leakage, which are utilized for statistical analysis⁸⁾. Recently, transmission electron microscopy (TEM) provided ultrastructural images, depicting the nanometer-sized water-filled spaces within the bonded interfaces through silver nitrate diffusion^{6,9)}. This silver deposition was quantitatively measured by image analysis; however, some representative positions were only selected for inclusion^{10,11)}. Scanning electron microscopy (SEM) also enabled to identify the silver uptake within the bonded interface, inducing an electron microscopic measurable contrast¹²⁻¹⁴⁾. Chang et al.¹³⁾ demonstrated that the water permeable interfaces might be indicative of weak positions for future degradation by SEM and also quantitatively compared silver infiltration among different adhesives by wavelength dispersive spectrometry (WDS). This study was designed to perform a quantitative comparison of the water-permeable zone in the adhesive and hybrid layer both before and after thermocycling among four commercial dentin adhesives to evaluate the bonding integrity. The first hypothesis tested in this study was that there was a difference in silver contents in the bonded interface among four commercial adhesives; and the second was that thermocycling leads to an increase in silver penetration within their interfaces.

II . MATERIALS AND METHODS

Specimen Preparation

Twenty eight freshly extracted human molars stored at 4°C in 0.5% chloramine-T solution were used. Flat dentin surfaces were created using a diamond saw (Isomet, Buehler, Lake Bluff, IL, USA). The exposed dentin was abraded with #500 silicon carbide paper. All specimens were randomly divided into four adhesive groups: OptiBond FL [OP] (Kerr,

Orange, CA, USA), AdheSE [AD] (Ivoclar-Vivadent, Schaan, Lichtenstein), Clearfil SE Bond [CL] (Kuraray, Osaka, Japan), and Xeno III [XE] (Dentsply, De Trey, Konstanz, Germany) (Table 1). Each specimen from four groups was bonded with one of the adhesives following the manufacturer's directions. One commercial composite resin (Premisa, Kerr, Orange CA, USA) was applied in 1 mm thickness and light-cured for 30 s with the equal intensity. After storage in distilled water at 4°C for 6 days each specimen was sectioned into halves occluso-gingivally perpendicular to the adhesive interface along its midpoint (Figure 1). Two parts of the tooth were divided into before and after thermocycling group, respectively. The former group specimens were sectioned to yield a 2 mm thick slab. The surface for examination was marked that it could confront the surface of its thermocycled counterpart, and then coated with nail varnish up to within 1 mm of the bonded interfaces. The specimens in the thermocycling group were subjected to 10,000 thermal cycles; i.e. changed between two water baths of 5°C and 55°C with a dwell time of 25 s and wait time of 5 s, respectively. After thermocycling, the specimen were sectioned to provide a 2 mm thick slab, and the surface for examination was confirmed to be adjacent to the surface of the tooth in the before thermocycling group and also coated with nail varnish in the same way. The specimens were blot dried and immediately immersed in a 50% ammoniacal silver nitrate solution (pH 9.5) for 24 h¹⁵⁾. The silver-stained specimens were rinsed in distilled water for 1 min and placed in a photo-developing solution (DS-76, Eastman Kodak Company, Rochester, NY, USA) for 8 h under a fluorescent light to facilitate reduction of silver ions into metallic silver particles. The surface for examination was ground and polished using wet silicone-carbide papers (#500, #1200) and diamond pastes with 6 μm, 3 μm, and 1 μm (DP-Paste, Struers A/S, Ballerup, Denmark) in a standardized way for each step and washed under the constant water stream for 2 min between polishing steps. For observation with SEM, the specimens were cleaned with a copious water stream, air dried, mounted on aluminum stubs and placed in a desiccator for 72 h.

SEM Examination with Chemical Analysis

For electron microscopic analysis, the specimens were coated with carbon using a sputter coater with carbon evaporation supply (BAL-TEC SCD 005 and CEA 035). For each specimen, the location where the silver penetrated was identified at 100× to 1000× magnification in a phase contrast of backscattered electron (BSE) mode of SEM (JEOL JSM-6380, Akishima, Japan) or electron probe micro analyzer

(EPMA: JEOL JXA-8900R, Akishima, Japan). The measurable silver contents were identified under WDS of EPMA, showing a positive correlation between silver contents and BSE brightness. On the image of each specimen, five lines were selected, each being perpendicular to the composite-dentin interface; the first line was 200 μm from the dentinoenamel junction and the last line was the same distance from the center of tooth (Figure 1). Another three scan lines run from the composite to the

Table 1. Materials used in this study

Product	Component (Batch No)	Composition	Application
OptiBond FL (Kerr, Orange, CA USA)	Prime (445404)	ethanol, Alkyl dimethacrylate, water	Etch for 15 s with 37.5% phosphoric acid (Kerr gel Etchant). Rinse for 15 s. Apply Prime and rub for 15 s. Dry for 5 s. Apply Adhesive in a uniform thin layer. Light cure for 30 s.
	Adhesive (446360)	Methacrylate ester monomers, Triethylene Glycol Dimethacrylate, Ytterbium Trifluoride, mineral fillers, initiators and stabilizers	
AdheSE (Ivoclar-Vivadent, Lichtenstein)	Self-Etch Primer (G12925)	DMA, Phosphonic acid acrylate, water, initiators and stabilizers	Apply Primer and brush it for 15 s. Air dry until the mobile liquid film is no longer visible. Apply Bond. Disperse Bond with a very weak stream of air. Light cure for 10 s.
	Adhesive(G12032)	HEMA, DMA, silicon dioxide, initiators and stabilizers	
Clearfil SE (Kuraray, Osaka, Japan)	Self-Etch Primer (00568B)	HEMA, 10-MDP, hydrophilic DMA, CQ, water, toluene	Apply Primer and leave it in place for 20 s. Evaporate the volatile ingredients with air. Apply bonding agent. Light cure for 10 s.
	Adhesive (00808A)	Silanated silica, Bis-GMA, HEMA, hydrophobic DMA, 10-MDP, CQ, toluene	
Xeno III (Dentsply, Detrey, Konstanz, Germany)	Self-Etch Primer & Adhesive (Liquid A 0601002833, Liquid B 0601002832)	Liquid A: HEMA, water, EthanolUrethane dimethacrylate, BHT, silicon dioxide Liquid B: Phosphoric acid modified polymethacrylate, Mono fluoro phosphazene modified methacrylate, Urethane dimethacrylate, BHT, CQ, Ethyl-4-dimethylaminobenzoate	Dispense equal amounts of Liquid A and Liquid B and mix it thoroughly for 5 s. Apply mixed adhesive and leave it undisturbed for 20 s. Light cure for 10 s.

Bis-GMA= bisphenol-A glycidyl dimethacrylate; BHT = butylated hydroxyl toluene; CQ = 1,7,7-Trimethylbicyclo-[2,2,1]-hepta-2,3-dione; DMA = dimethacrylate; HEMA= 2-hydroxyethylmethacrylate; 10- MDP = 10-methacryloyloxydecyl dihydrogen phosphate

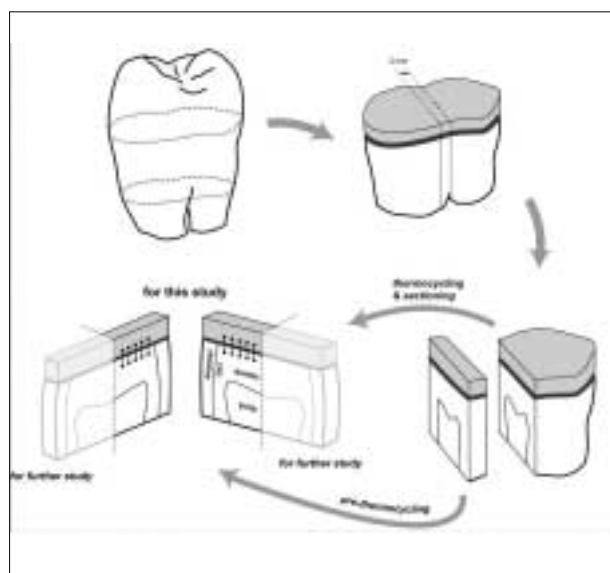


Figure 1. Diagram for specimen preparation.

dentin, maintaining the same distance to each other, only except when they avoided artifacts such as voids. A silver element was the primary indicator for dye penetration, whereas Si and Ca were selected for the secondary indicators of composite and dentin. The values measured for each 0.2 μm interval were averaged into a single value per each scan line. The unit of value was the intensity of the characteristic x-ray per 200 msec, which indicated the relative contents of elements. Operating conditions for both the image and elemental analysis of EPMA were 15 kV accelerating voltage, 50 nA beam current and focused beam mode (\diamond 1 μm beam diameter).

Statistical analysis and sample size justification

While inter-location differences were not significant, inter-specimen differences were statistically significant ($p < 0.0001$), which suggested that consideration of the individual difference among specimens was inevitable. Therefore, a mixed-level repeated measures analysis of variance (ANOVA) and a mixed-level repeated measures analysis of covariance (ANCOVA) were used to compare silver contents within four types of dentin adhesives before and after thermocycling, respectively, under consideration of five correlated measurements from the same specimen and differences among specimens¹⁶⁾. Silver contents within four dentin adhesives before

and after thermocycling were compared separately, and their comparison after thermocycling was performed under adjustment for silver contents before thermocycling as a covariate. Comparison of silver contents between two stages in the same specimen was analyzed by paired t-test. Using the Mixed Procedure of SAS statistical package version 9.13, the analysis of 28 molars had approximately 87% power to detect a 2.0 SD difference between any two groups at any of the five locations at a significance level of 0.05.

III. RESULTS

Elemental analysis showed individual distribution of each element, and it was possible to clarify distinct borders in the dentin-hybrid-adhesive-composite layer (Figures 2a and 2b). The adhesive layer begins at the point where the silica contents drop significantly and ends at the point where calcium, which is the representative element of dentin, increases. The hybrid layer starts from the point where calcium apparently increases and ends at the point where silica disappears. The horizontal scales determine the distance of the scan line across the adhesive interface. The vertical scales are the relative weight value of each element. There was a slight rise in silver content in the adhesive layer, while Si contents decreased because the adhesive contained fewer amounts of fillers than the composite. The silver content infiltrated the adhesive layer and the hybrid layer was obtained, respectively. Before thermocycling, in the adhesive layer, OP showed the lowest silver uptake, followed by CL, AD, and XE in ascending order ($p < 0.0001$); in the hybrid layer, CL was the lowest among four groups ($p = 0.0039$, Table 2). After thermocycling, in the adhesive layer, OP showed the lowest silver uptake, followed by CL, AD, and XE in ascending order ($p < 0.0001$); in the hybrid layer, XE was the highest among four groups ($p = 0.0014$). Comparing before and after thermocycling, in the adhesive layer, no group manifested a significant difference in silver content and showed a slight decrease except XE, which presented a small increase. In the hybrid layer most had the same tendency toward a decrease and only AD showed a sig-

nificant decrease ($p = 0.0367$).

SEM revealed cross-sectional interfaces of before and after thermocycling counterparts. For OP, there was relatively uniform deposition of silver along the hybrid layer and no distinguishable change was observed after thermocycling (Figures 3a, 3b and 3c). Many specimens in the AD group suffered dehydration stress from the high vacuum of SEM and manifested artifactual fracture between the adhesive and hybrid layer (Figures 4a and 4b). Also silver particles coalesced and formed droplets within the

adhesive layer. For CL, silver uptake represented by a thin white line was shown along the hybrid layer, and bonding of the integrity between the adhesive and hybrid layer was maintained throughout thermocycling (Figures 5a and 5b). XE was marked by a densely white band overall on the interface, regardless of the adhesive and hybrid layer, which extended up to the enamel margin (Figures 6a and 6b). After thermocycling, silver particles were demonstrated by irregular coagulum of a thick electro-dense image (Figure 6c).

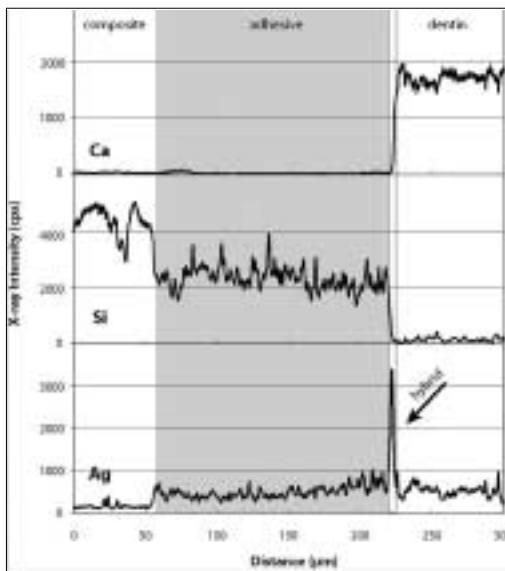


Figure 2 a. Elemental analysis of silver (Ag), calcium (Ca), and silica (Si) on an immediate bonding specimen in OptiBond FL group. Note the sharp peak of Ag as demonstrated in the hybrid layer (arrow) where the Ca value started to rise as well.

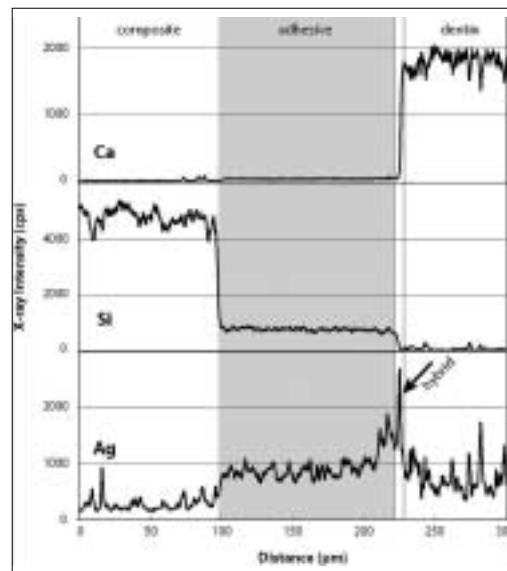


Figure 2 b. An immediate bonding specimen in the Clearfil SE Bond group. Note the increase of Ag in the adhesive layer. The Si level of the adhesive is lower than that in OP because of their different filler composition.

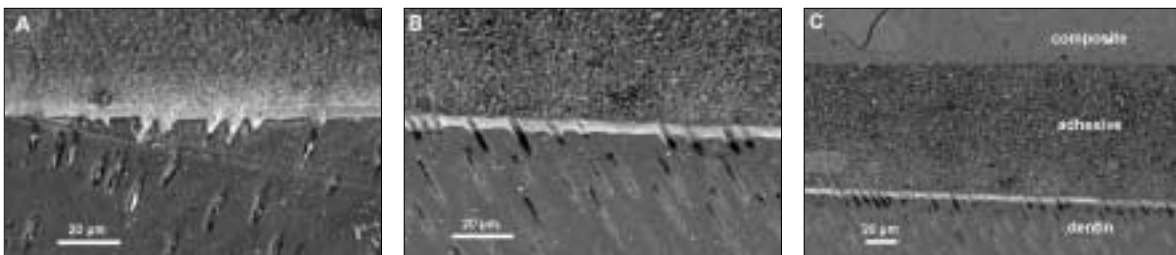


Figure 3. OptiBond FL: (a) SEM micrograph with 1000 \times magnification of the initial bonding status before thermocycling. Silver uptakes were represented by a dense white image in the hybrid layer and dentinal tubules (b) After thermocycling. SEM showed the adjacent location to where the picture (a) was taken. Silver penetration occurred in a similar pattern. (c) SEM of the same location as (b) with a lower magnification. Integrity of bonding seemed to be maintained between composite resin and dentin throughout thermocycling.

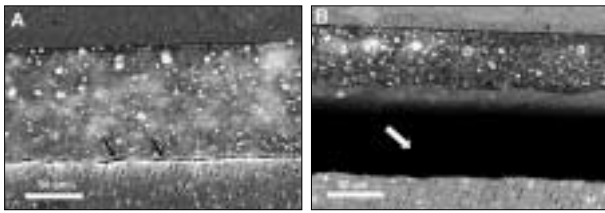


Figure 4. AdheSE: (a) Before thermocycling. Multiple silver droplets were contained within the adhesive layer. Artfactual crack line from vacuum stress was demonstrated right above the hybrid layer (arrows). (b) The adjacent area after thermocycling. Crack propagated further between the adhesive and hybrid layer (white arrow). There was no change in silver accumulation patterns.

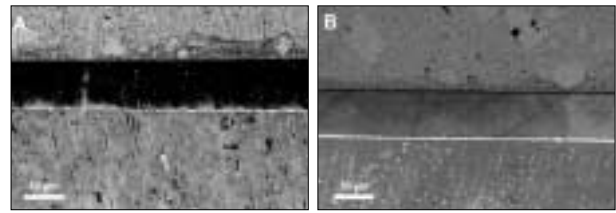


Figure 5. Clearfil SE Bond: (a) Before thermocycling. Silver mostly presented in the thin hybrid layer. (b) The area next to (a) after thermocycling. Bonding interface kept integrated with the silver penetrated hybrid layer in the same manner.

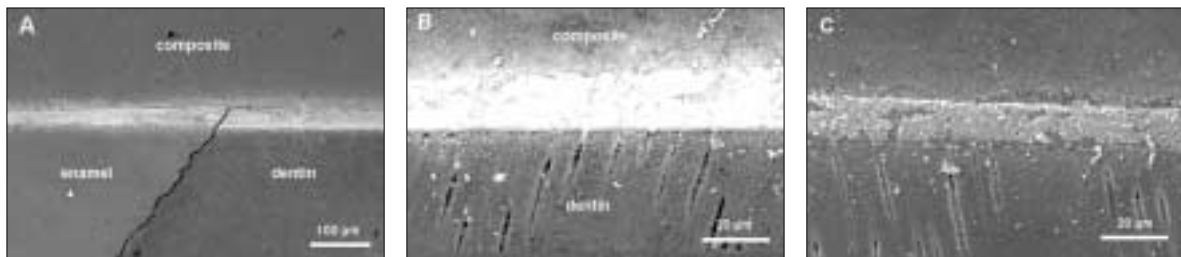


Figure 6. Xeno III [XE] (a) Bonding before thermocycling. It is noticeable that silver penetration occurred in composite/enamel interface as well as in composite/dentin and appeared overall in the adhesive and hybrid layer. (b) Before thermocycling. Dense deposition of silver was spread uniformly along the adhesive and hybrid layer. (c) The adjacent location was shown after thermocycling. Silver particles coalesced in an irregular form.

Table 2. Relative mean silver contents within four types of dentin adhesives before and after thermocycling under consideration of multiple measurements of the specimen

Adhesive type (OP)	Optibond FL (AD)	Adhe SE (CL)	Clearfil SE (XE)	Xeno III	p - value
Adhesive layer					
Before thermocycling	1708(1065) ^a	3027(1444) ^b	2262(1007) ^c	4560(1420) ^d	<0.0001
After thermocycling [†]	1621(1305) ^a	2396(831) ^b	2214(815) ^b	4819(1233) ^c	<0.0001
p-value	0.6449	0.094	0.7693	0.4562	
Hybrid layer					
Before thermocycling	4194(1327) ^a	4237(1413) ^a	3699(1442) ^b	4643(1060) ^a	0.0039
After thermocycling [†]	3785(1297) ^a	3201(1467) ^a	3575(1001) ^a	4496(899) ^b	0.0014
p-value	0.2596	0.0367	0.6747	0.4599	

Means and standard deviations in parentheses. Different letters in the same row mean statistically significant differences at significance level 0.05.

[†] Silver contents after thermocycling were compared under adjustment for silver contents before thermocycling.

IV. DISCUSSION

Microscopic evaluation of the leakage often accompanies a destructive methodology. In most degradation tests, teeth are randomly assigned to various experimental groups and exclusively subjected to a corresponding test. To overcome the individual tooth difference and the regional variance within a dentin substrate, a large number of specimens are needed to gain statistical relevance¹⁷. In this study, to assess the individual tooth difference, the magnitude of correlation among multiple measures of silver contents from a specimen was obtained by the intraclass correlation (ICC), represented as, $ICC = \sigma_b^2 / (\sigma_b^2 + \sigma_e^2)$, in which σ_b^2 and σ_e^2 denoted between-specimen variance and within-specimen variance, respectively (in the adhesive layer, immediate bonding = 0.29, thermocycled = 0.25; in the hybrid layer, immediate bonding = 0.37, thermocycled = 0.23). This is similar to Eckert et al.'s result obtained from a microtensile bond strength test, in which the overall correlation between beams was 0.27¹⁷. Considering the expected correlation within the specimen, this study attempted to perform a paired test by using two adjacent sections that originated from the same tooth. Each section belonged to a separate experimental group and had a mirror image resembling the surface to be observed with SEM. Both surfaces were compared to determine the change occurred through the aging process simulated by thermocycling. Not only were silver penetration patterns obtained, but also silver contents were quantitatively measured and statistically analyzed. In this light, this study differed from previous studies, which usually compared the area where dye was infiltrated^{11,18}. Five scan lines were drawn in a standardized way to represent the interface between composite resin and dentin. Micrographs were taken for comparison at the same location in specimens of both stages (Figures 3 - 6).

Before thermocycling OP, a three-step etch and rinse system showed the least silver uptake in the adhesive layer. Its separate bottle of adhesive is comprised of hydrophobic monomers, which makes it less prone to water penetration¹⁹. And OP was loaded with a relatively larger amount of fillers, considering

that more silica was detected in the adhesive layer, compared with other systems (Figure 2a). In AD and CL, two-step self-etch adhesive systems, the hydrophobic adhesive was also applied onto the self-etched dentin. However, the silver contents of both systems were significantly different from each other (Table 2) and also demonstrated dissimilar characteristics of penetration in the micrographs (Figures 4a and 5a). This may be due to the different functional monomers contained in their respective systems. Bisphenol-A-glycidyl methacrylate (Bis-GMA) in CL, which serves as a cross-linking backbone in the polymer structure, is less soluble compared to other forms of dimethacrylate²⁰. Another ingredient, 10-methacryloyloxydecyl dihydrogen phosphate (10-MDP) is known to intimately interact with calcium salts from hydroxyapatite crystals^{21,22}. This may be correlated to the well-retained, intact interface, even under the high vacuum of SEM (Figures 5a and 5b) and the lower silver content within the hybrid layer (Table 2). One-step self-etch, XE, which demonstrated the most silver uptake, showed a very dense accumulation of silver overall in the interface, such that the adhesive and the hybrid layer were hardly demarcated (Figure 6a). This may have been caused by the hydrophilic nature of the all-in-one system that was comprised of mixture of acidic monomers with an aqueous solvent (Table 1). Therefore, our first hypothesis was accepted.

The hybrid layer was distinguished by a high peak of silver (Figures 2a and 2b), consistent with the quantitative assessment of this study (Table 2). This area was governed by the hydrated dentin substrate and also served as a water reservoir below the hydrophobic barrier. It has often brought into a question where the weakest link would be in the interface joining the composite resin, artificial restorative material and the dentin, biological tissue. Commonly, the most susceptible position is regarded as the area right above the hybrid layer, which is saturated with more water than the next layer. Our study showed that the water-bearing area contributed to artifactual failure under the dehydration stress (Figures 4a and 4b). In other aspects, the fracture topography in previous studies often demonstrated the mixed fracture mode, implying that stress concentration happened

from the intra-structural defects within the adhesive layer^{7,23)}. Also, in a longitudinal section a cohesive fracture mode within the adhesive layer was well presented by SEM when hydrophilic adhesives were used¹³⁾. Furthermore, incompatibility between chemically-cured composite resins and simplified-step adhesives was reported to occur, because their bonding failure above the adhesive layer was partially due to the water movement across the permeable adhesive during a slow polymerization period^{24,25)}. Therefore, any water-bearing spots or pores in a resinous structure seemed to create flaws in the bonding integrity. This study used a light-cured composite resin which provided the hydrophobic barrier immediately after light activation. However, SEM pictures demonstrated water droplets which were continuously transformed across the polymerized adhesive layer (Figures 4a and 6a).

The effect from the artificial aging process by thermocycling was supposed to threaten the hydrolytic stability of the polymer network and to extract poorly polymerized resin oligomers⁷⁾. This study applied 10,000 cycles, which was suggested for one service year²⁶⁾. For a paired test, a sectioned specimen was directly exposed to the changing environment. Water-induced polymer degradation within the interface was readily expected; however, the SEM was unable to determine any significant changes in a counterpart specimen after thermocycling (Figures 3b, 3c, 4b, 5b, and 6c). Consistent with these findings, there was also no significant increase in silver uptake. Only XE showed a slight increase of silver in the adhesive layer, while other cases rather presented a small decrease (Table 2). In the hybrid layer of AD, there was a significant decrease in silver uptake. Some amount of silver loss might be expected from the artifactual fracture during the SEM test. So, our second hypothesis was not accepted.

There are several other assumptions behind our results. It may be that tracer penetration assured by microscope is not directly linked to gap dimensions, particularly in water swollen materials^{26,27)}. Another contributing factor can be the alkaline nature of silver nitrate. The hydroxyl ions exerted from ammoniacal silver nitrate could accelerate the hydrolysis of

the polymer structure, mimicking an aged degradation²⁸⁾. Hence, some area occupied by silver was assumed to be in the voids produced by the dissolved matrix, filler particles, and the interfacial-coupling agent²⁹⁾. This space might be already created in an initial bonding stage, and correspond to the vulnerable position to a future aging phenomenon. In this case, thermocycling does not further damage to an already defective interface^{29,30)}. Future study needs to be designed for the alkaline effect of trace material excluded. In this study, water permeable region confirmed by a microscopic tool indicated hydrolysis susceptible area. Increased permeability within the bonding interface may compromise the structural integrity and this might be negatively related to the clinical longevity.

V. Conclusion

Four commercial dentin adhesive systems manifested different silver uptake in the adhesive and hybrid layer with characteristic patterns of infiltration. Their different compositions seemed to provide varied permeability in a hydrous environment. Thermocycling did not increase the silver penetration of the bonded interfaces.

REFERENCES

1. Opdam NJ, Bronkhorst EM, Roeters JM, Loomans BA. A retrospective clinical study on longevity of posterior composite and amalgam restorations. *Dent Mater* 23(1):2-8, 2007
2. da Rosa Rodolpho PA, Cenci MS, Donassollo TA, Loguercio AD, Demarco FF. A clinical evaluation of posterior composite restorations: 17-year findings. *J Dent* 34(7):427-435, 2006.
3. Kramer N, Garcia-Godoy F, Reinelt C, Frankenberger R. Clinical performance of posterior compomer restorations over 4 years. *Am J Dent* 19(1):61-66, 2006.
4. Manhart J, Chen H, Hamm G, Hickel R. Buonocore Memorial Lecture. Review of the clinical survival of direct and indirect restorations in posterior teeth of the permanent dentition. *Oper Dent* 29(5):481-508, 2004.
5. De Munck J, Van Landuyt K, Peumans M, Poitevin A, Lambrechts P, Braem M, et al. A critical review of the durability of adhesion to tooth tissue: methods and results. *J Dent Res* 84(2):118-132, 2005.
6. Tay FR, King NM, Chan KM, Pashley DH. How can nanoleakage occur in self-etching adhesive systems that demineralize and infiltrate simultaneously? *J*

- Adhes Dent* 4(4):255-269, 2002.
7. De Munck J, Van Landuyt K, Coutinho E, Poitevin A, Peumans M, Lambrechts P, et al. Micro-tensile bond strength of adhesives bonded to Class-I cavity-bottom dentin after thermo-cycling. *Dent Mater* 21(11):999-1007, 2005.
 8. Tulunoglu O, Uctasli MB, Ozdemir S. Coronal microleakage of temporary restorations in previously restored teeth with amalgam and composite. *Oper Dent* 30(3):331-337, 2005.
 9. Hiraishi N, Breschi L, Prati C, Ferrari M, Tagami J, King NM. Technique sensitivity associated with air-drying of HEMA-free, single-bottle, one-step self-etch adhesives. *Dent Mater* 23(4):498-505, 2007.
 10. Reis AF, Bedran-Russo AK, Giannini M, Pereira PN. Interfacial ultramorphology of single-step adhesives: nanoleakage as a function of time. *J Oral Rehabil* 34(3):213-221, 2007.
 11. Reis AF, Giannini M, Pereira PN. Long-term TEM analysis of the nanoleakage patterns in resin-dentin interfaces produced by different bonding strategies. *Dent Mater* 23(9):1164-72, 2007.
 12. Yuan Y, Shimada Y, Ichinose S, Tagami J. Qualitative analysis of adhesive interface nanoleakage using FE-SEM/EDS. *Dent Mater* 23(5):561-9, 2007.
 13. Chang J, Platt JA, Yi K, Cochran MA. Quantitative comparison of the water permeable zone among four types of dental adhesives used with a dual-cured composite. *Oper Dent* 31(3):346-353, 2006.
 14. Akimoto N, Yokoyama G, Ohmori K, Suzuki S, Kohno A, Cox CF. Remineralization across the resin-dentin interface: in vivo evaluation with nanoindentation measurements, EDS, and SEM. *Quintessence Int* 32(7):561-570, 2001.
 15. Pashley EL, Agee KA, Pashley DH, Tay FR. Effects of one versus two applications of an unfilled, all-in-one adhesive on dentine bonding. *J Dent* 30:83-90, 2002.
 16. RC L. SAS System for Mixed Models. Cary, NC: SAS Institute Inc :171-227, 1996.
 17. Eckert GJ, Platt JA. A statistical evaluation of microtensile bond strength methodology for dental adhesives. *Dent Mater* 23(3):385-391, 2007.
 18. Reis A, Grande RH, Oliveira GM, Lopes GC, Loguercio AD. A 2-year evaluation of moisture on microtensile bond strength and nanoleakage. *Dent Mater* 23(7):862-70, 2007.
 19. 최승모, 박상혁, 최경규, 박상진. 중간층 레진 적용이 단일 접착 과정 상아질 접착제의 접착에 미치는 영향. *대한치과보존학회지* 32:313-326, 2007.
 20. Moszner N, Salz U, Zimmermann J. Chemical aspects of self-etching enamel-dentin adhesives: a systematic review. *Dent Mater* 21(10):895-910, 2005.
 21. Gueders AM, Charpentier JF, Albert AI, Geerts SO. Microleakage after thermocycling of 4 etch and rinse and 3 self-etch adhesives with and without a flowable composite lining. *Oper Dent* 31(4):450-455, 2006.
 22. Inoue S, Koshiro K, Yoshida Y, De Munck J, Nagakane K, Suzuki K, et al. Hydrolytic stability of self-etch adhesives bonded to dentin. *J Dent Res* 2005;84(12):1160-1164.
 23. Monticelli F, Osorio R, Pisani-Proenca J, Toledano M. Resistance to degradation of resin-dentin bonds using a one-step HEMA-free adhesive. *J Dent* 35(2):181-186, 2007.
 24. Tay FR, Suh BI, Pashley DH, Prati C, Chuang SF, Li F. Factors contributing to the incompatibility between simplified-step adhesives and self-cured or dual-cured composites. Part II. Single-bottle, total-etch adhesive. *J Adhes Dent* 5(2):91-105, 2003.
 25. Cheong C, King NM, Pashley DH, Ferrari M, Toledano M, Tay FR. Incompatibility of self-etch adhesives with chemical/dual-cured composites: two-step vs one-step systems. *Oper Dent* 28(6):747-755, 2003.
 26. Gale MS, Darvell BW. Thermal cycling procedures for laboratory testing of dental restorations. *J Dent* 27(2):89-99, 1999.
 27. Tae-Yeon Lee, Byeong-Hoon Cho, Ho-Hyun Son, 상아질 접착제의 nanoleakage 양상에 관한 연구, *대한치과보존학회지* 28:169-177, 2003.
 28. Sarkar NK. Internal corrosion in dental composite wear. *J Biomed Mater Res* 53(4):371-380, 2000.
 29. Bagheri R, Tyas MJ, Burrow MF. Subsurface degradation of resin-based composites. *Dent Mater* 23(8):944-51, 2007.
 30. 문영훈; 김종률; 최경규; 박상진, 열순환이 상아질 접착제의 결합 내구성에 미치는 영향, *대한치과보존학회지* 32:222-235, 2007.

국문초록

열순환 후 상아질 접착 계면의 수분 투과성 변화에 대한 정량적 분석

장주혜¹ · 이기욱² · 김혜영³ · 이인복¹ · 조병훈¹ · 손호현^{1*}

¹서울대학교 치의학대학원 치과보존학교실, ²한국기초연구과학지원연구원

³서울대학교 치의학생명과학사업단 (BK 21)

본 연구는 현재 시판 되고 있는 여러 개의 상아질 접착제를 임상 술식에서와 같은 방법으로 사용한 다음 열순환 후 접착계면의 변화를 관찰 비교하고자 했다.

발거 한 지 한 달 이내인 대구치 28개의 교합 면 상아질 표면에 4종의 상아질 접착제 (OptiBond FL [OP], AdheSE [AD], Clearfil SE Bond [CL], Xeno III [XE] 중 하나를 적용한 뒤 복합 레진 (Premisa, Kerr) 을 1 mm 두께로 올린 후 광중합 하였다. 4°C 증류수에서 6일간 보관한 뒤, 치아의 정중선으로부터 수직으로 절단 하여 그 중 절반의 치아에서 2 mm 두께의 시편을 얻은 다음 남은 반쪽의 치아는 10,000회의 열순환을 가한 뒤 (5°-55°, 침지 시간 25초, 대기 시간 5초) 같은 방법으로 2 mm 두께의 시편을 얻었다. 연마한 시편을 24시간 동안 50% ammoniacal silver nitrate solution에 담근 다음 photo-developing solution에서 8시간 동안 환원시켰다. 계면을 가로지르는 5개의 line 상에서 wavelength dispersive spectrometry (WDS) detector를 이용하여 주사선상에 있는 원소들의 중량비를 계산하였다. 또한 열순환 전과 후의 시편에서 얻어진 5개의 silver 측정치를 서로 비교하였다.

열순환 전의 접착제층(adhesive layer)에서는 OP 에서 가장 적은 silver의 투과가 관찰되었으며 ($p < 0.0001$), CL, AD, XE 순으로 투과 량이 증가함을 보였다. 혼성층 (Hybrid layer) 에서는 CL의 투과량이 가장 적었다 ($p = 0.0039$). 열순환 후에 접착제층과 혼성층에서 silver의 투과량은 증가하지는 않았다. Scanning electron microscopy (SEM) 사진을 통하여 각 시편의 접착 계면에서 접착제에 따른 특이적인 silver의 투과상을 관찰할 수 있었다. 전반적으로 OP 와 CL의 접착계면이 열순환 과정 중에도 온전히 유지됨을 볼 수 있었다.

접착 계면에서의 수분 투과 양상은 각 접착제에 따라 다른 형태를 보였으며 열 순환에 의해 유의할 만한 변화를 야기하지는 않았다.

주요단어 : 상아질, 접착제, SEM, WDS, 열순환 처리, 수분 투과성